Journal of New Trends in Sciences
Volume. 3, Nomor. 4 November 2025
e-ISSN : 2964-1624; P-ISSN : 2964-1799; Hal 42-58
DOI : https://doi.org/10.59031/jnts.v3i4.740
Tersedia: https://jurnal.aksaraglobal.co.id/index.php/jnts

Advancing Renewable Energy Materials: Corrosion and Strength Optimization of 17-4 PH Stainless Steel for Geothermal Turbines

Muhammad Alvito Faros [1*], Riri Murniati [2], Agus Hadi Santosa Wargadipura [3]
[1,2] Study Program of Physics, Indonesia Defense University, IPSC Sentul, Bogor, 16810
[3]Advanced Materials Research Center, National Research and Innovation Agency (BRIN), Banten, 15314

Alamat: Study Program of Physics, Indonesia Defense University, IPSC Sentul, Bogor, 16810
Korespondensi penulis: muhammadalvitofaros@gmail.com

Abstract. *This research explores the engineering and performance evaluation of 17-4 PH stainless steel as a potential material for turbine blades in geothermal power plants (PLTP). To promote renewable energy innovation in industrial engineering, this study focuses on improving material reliability through microstructural optimization and mechanical property control. The material was produced using the investment casting method at PT SPVMB and then subjected to four heat treatment variations: H900, H1025, AVG (average), and as-cast conditions, with reference to ASTM A747 standards. Mechanical and corrosion characterization were performed through hardness and tensile tests, electrochemical corrosion analysis using geothermal water from the Dieng PLTP, and microstructural observation using an optical microscope. The results showed that the H900 condition had the highest hardness and yield strength (48.46 HRC and 939.25 MPa), but its corrosion rate was relatively high. In contrast, the H1025 heat treatment provides balanced mechanical strength (43.88 HRC and 860.91 MPa) with the lowest corrosion rate (0.027 mm/year), supported by a uniform tempered martensite structure. These findings indicate that heat treatment optimization significantly improves the suitability of 17-4 PH stainless steel for sustainable geothermal applications. The H1025 condition meets all the requirements for geothermal turbine blades, including hardness, strength, and corrosion resistance, potentially extending component life and reducing maintenance costs. Furthermore, the results of this study strengthen the agenda for developing durable, environmentally friendly materials to support renewable energy systems. This study also provides practical insights for industry in selecting the optimal heat treatment that combines mechanical performance and corrosion resistance in extreme geothermal environments.*

Keywords: *17-4 PH stainless steel, corrosion resistance, geothermal, heat treatment, mechanical strength.*

1. INTRODUCTION

Energy is a resource used for various activities, such as fuel, electricity, mechanical energy, and heat. This energy comes from energy sources, which are anything capable of producing energy, either directly or through a transformation or conversion process. Energy sources themselves are part of natural resources, including oil and natural gas, coal, water, geothermal energy, peat, biomass, and others, which can be used directly or indirectly as energy (Azhar & Adam Satriawan, 2018).

The rapid transition from fossil fuels to renewable energy sources, such as geothermal energy, is becoming increasingly urgent due to the worsening climate crisis and the limited availability of fossil fuels. The Intergovernmental Panel on Climate Change (IPCC) has emphasized that to prevent severe environmental consequences, global warming must be kept below 1.5°C, which means the immediate implementation of low-carbon energy systems

Received Maret 28, 2025; Revised Juli 11, 2025; Accepted Juli 25, 2025; Publish Agustus 8, 2025
** Muhammad Alvito Faros, muhammadalvitofaros@gmail.com*

(IPCC, 2018). Fossil fuels contribute more than 70% of global greenhouse gas emissions, accelerating climate change, polluting the air, and depleting natural resources (IEA, 2021).

Geothermal energy is a reliable, sustainable energy option because it can provide continuous electricity with very low emissions. This makes it an ideal solution, especially in areas rich in geothermal potential. Unlike solar or wind energy, which are dependent on weather conditions, geothermal energy can produce power consistently, thus strengthening energy security and helping achieve global decarbonization targets (Bertani, 2016).

Geothermal energy is a type of renewable energy derived from heat stored within the Earth's crust. Indonesia has significant geothermal resource potential, with characteristics generally categorized as medium to high enthalpy. This potential makes geothermal energy a viable alternative for generating electricity, playing a crucial role in supporting the increase in electrification rates throughout Indonesia (Afriandi & Hantoro, 2018).

Indonesia has abundant geothermal resources originating from both volcanic and non-volcanic activity, totaling 276 locations. According to the 2008–2027 National Electricity General Plan, Indonesia's geothermal energy potential is estimated at 27.5 GWe. This makes Indonesia the country with the largest geothermal reserves in the world, accounting for approximately 40% of the total global potential, spread across 256 locations throughout the country (Trisakti et al., 2020).

Geothermal power plants typically exhibit lower efficiency (~10–13%) compared to conventional thermal plants, largely due to fluid enthalpy limitations and thermodynamic constraints (Zarrouk, 2014). While geothermal energy benefits from low operational costs and continuous availability, its upfront capital expenditure is substantial frequently estimated at USD 3,000–6,000 per kW (≈ $3–6 million per MW)—leading to levelized cost of electricity (LCOE) values typically in the range of USD 60–73/MWh (Blecich, 2021). Encouragingly, more recent IRENA data suggest that LCOE for new geothermal projects collectively dropped to around USD 56/MWh in 2022 making geothermal increasingly competitive with other renewables. However, capital costs remain comparatively high in most regions, and technology deployment is still constrained by site-specific resource variability. In contrast, onshore wind and utility-scale solar now achieve much lower LCOE values—averaging USD 33–49/MWh—according to IRENA 2022 data (Wyszomierksi, 2025). Despite the higher initial cost of geothermal, its capacity factor is far superior often exceeding 80–90 % compared to ~35 % for wind and ~25 % for solar making geothermal a dependable baseload source with high utilization (Kabeyi, 2021).

The use of geothermal energy for electricity generation in Indonesia began in the 1980s, with the operation of the Kamojang Unit I Geothermal Power Plant (PLTP) in February 1983, which has a capacity of 30 Megawatts. Based on the National Energy General Plan (RUEN), it is targeted that by 2025 the electricity contribution from PLTP will reach 7.2 Gigawatts nationally. However, until now the development of geothermal energy is still relatively minimal, even though the geothermal potential in Indonesia is estimated to reach 28.5 Gigawatts. As of September 2018, the utilization of geothermal energy has only reached 1,948.5 Megawatts spread across 12 PLTPs throughout Indonesia (M. Batubara, 2018).

The vast geothermal potential in a volcanic country like Indonesia, if maximized, will not only support national resilience but also become a key driver in the global decarbonization strategy. To support the optimal use of geothermal energy, a reliable and durable generation system is required, particularly for critical components such as turbines.

Turbine blades are a crucial component in geothermal power plants, driving the generator through geothermal steam pressure directed to the turbine blades. This geothermal steam contains various corrosive chemical compounds, such as Hydrogen Sulfide (H_2S), Carbon Dioxide (CO_2), Ammonia (NH_2), Chloride (Cl^-), and Sulfate (SO_4 $^{2-}$), which can corrode turbine blade materials over time (Karlsdottir et al., 2015). Therefore, the materials used must have high corrosion resistance, be able to withstand extreme temperatures, and have strong mechanical properties to withstand harsh operational conditions (Yamamoto et al., n.d.).

H_2S accelerates the degradation of the passive film, generating brittle ferrous sulfide (FeS, FeS_2) and increasing the risk of sulfide stress cracking, especially under internal stress (Iglesias et al., 2025). CO_2 forms carbonic acid in water, lowering the pH and triggering uniform corrosion and pitting through the formation of $FeCO_3$, which becomes more aggressive at high temperatures (>120°C) (Aristia, 2025).

Chloride ions (Cl^-) are known to be the primary trigger for pitting corrosion in stainless steel because they can penetrate the Cr_2O_3 passive layer, causing local depassivation and the formation of rapidly growing corrosion pits (Penot, 2023).

17-4 PH stainless steel is a type of martensitic stainless steel that undergoes precipitation hardening, has high strength like martensitic stainless steel and excellent corrosion resistance like austenitic stainless steel. Many important components in industrial applications, such as jet engine components, gears, chemical process equipment, nuclear reactor components and decks are produced by this material (Karthik et al., 2015).

The heat treatment process significantly affects the mechanical properties of SS 17-4 PH stainless steel, as it influences microstructural transformations, including phase changes,

precipitation hardening, and grain refinement. The selection of heat treatment parameters, such as solution treatment temperature, aging temperature, and cooling rate, determines the ultimate strength, hardness, and toughness of the material, which are critical for high-performance applications such as geothermal power plant turbine blades. Proper heat treatment promotes the precipitation of Cu-rich phases, improving strength and corrosion resistance, while inadequate treatment can lead to undesirable phases that reduce material performance (Sabooni et al., 2021).

Previous research from Mahmoudi & Elwani in 2017 has shown significant variations in tensile strength and corrosion rate depending on fabrication method and heat treatment cycle. However, the studies have used fabrication methods such as rolling and selective laser melting, as well as artificial corrosion media.

Table 1. Heat Treatment Cycle Variation Data

Condition	***Treatment***
H900 (A)	1050 °C × 0.5 h → *air cool* → 482 °C × 1 h → air cool *(ASTM A747 Standard)*
AVG (B)	1050 °C × 0.5 h → *air cool* → 515 °C × 2.5 h → *air cool (Median)*
H1025 (C)	1050 °C × 0.5 h → *air cool* → 550 °C × 4 h → air cool *(ASTM A747 Standard)*
As Cast (D)	*No heat treatment applied (Directly from investment casting process)*

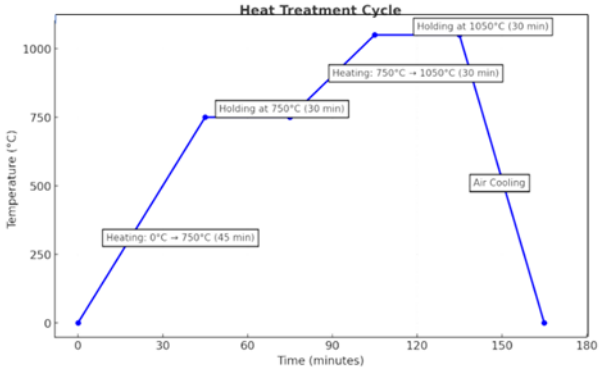

Figure 1. Heat Treatment Annealing Cycle

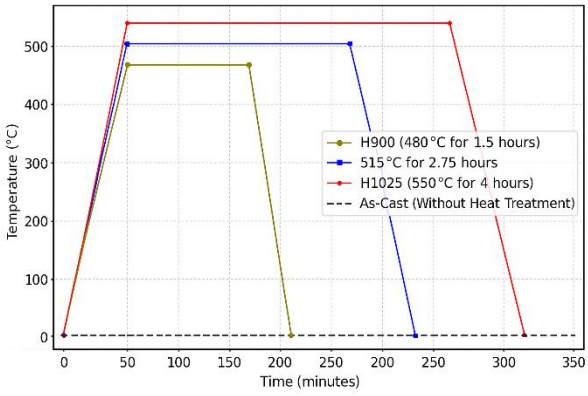

Figure 2. Heat Treatment Tempering Cycle

Unlike previous works that relied on artificial corrosion media and different fabrication method, this study uses real geothermal brine and investment casting, reflecting actual field condition.

This study aims to evaluate the performance of 17-4 PH investment casting stainless steel heat-treated according to ASTM A747 standards, namely conditions H900, H1025, and one intermediate variation (AVG). The evaluation includes hardness tests, tensile tests, electrochemical corrosion analysis in original brine solution from the Dieng Geothermal Power Plant, and microstructural observations. The results of the study are expected to determine optimal heat treatment conditions that increase efficiency, extend service life, support national energy security and reducing import dependence in indonesia's geothermal sector through the development of local materials for geothermal turbine components. Second, by performing electrochemical corrosion analysis using real geothermal brine from the Dieng Geothermal Powerplant, this study offers a realistic evaluation of material performance in the complex and aggresive environtment of geothermal turbine. Ultimately, this research aims to contribute to the advancement of sustainable geothermal energy technology in Indonesia by identifying heat treatment strategies that optimize the mechanical and corrosion performance of locally produced 17-4 PH stainless steel turbine blades, thereby enhancing durability, reducing reliance on imports, and supporting the country's national energy security goals.

2. RESEARCH METHOD

Design, Place and Time

This study uses an experimental quantitative approach to evaluate the effect of heat treatment variations on the mechanical properties, corrosion resistance, and microstructure of 17-4 PH stainless steel resulting from the investment casting process. The study was conducted at the Advanced Materials Research Center, BRIN (Building 224 KST B.J. Habibie, Serpong)

from January to April 2025. The research series includes heat treatment processes, mechanical testing, microstructural observations, and corrosion tests in geothermal brine solutions.

Quantity and Method of Obtaining Materials and Equipment (Laboratory)

The research samples consisted of 12 SS 17-4 PH steel bars for tensile testing, 4 coin samples for hardness testing, and 4 other coins for corrosion testing. The materials were obtained from investment casting and prepared according to testing standards. The main equipment used included a Nabertherm furnace for heat treatment, a 250 kN UTM machine for tensile testing, a Brinell Hardness Tester machine for hardness testing, an Olympus CX-31 optical microscope for microstructural observation, and a Parstat 4000A corrosion test device for electrochemical corrosion analysis.

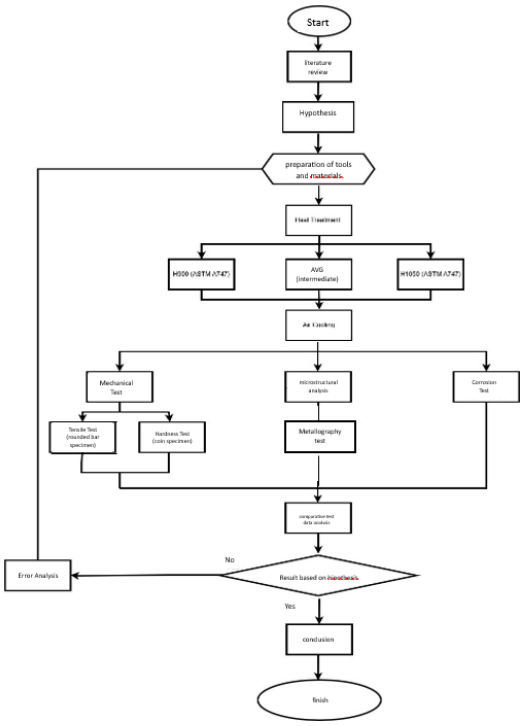

Figure 3. Research methodology

Types and Methods of Data Collection / Research Stages (Laboratory)

The research process began with heat treatment using three variations: H900, AVG, and H1025, following the ASTM A747 standard. The process began with solution annealing at a temperature of 1050°C for 30 minutes, ending with air cooling. Next, the tempering process was carried out according to the various conditions and also closed with air cooling. The next stages included hardness testing using the Brinell method (ASTM E10), tensile testing

according to ASTM E8, and microstructural observation through metallographic techniques (grinding, polishing, and etching) using a $CuCl_2$-HCl-Aquades solution.

Corrosion tests were conducted using two methods, namely Open Circuit Potential (OCP) for 30 minutes and Potentiodynamic Polarization at a scan rate of 1 mV/min using original brine solution from the Dieng Geothermal Power Plant. Data were obtained from the results of corrosion potential measurements (Ecorr), corrosion current density (Icorr), and corrosion rate, which were calculated based on the Tafel curve.

Data Processing and Analysis

The test data were analyzed quantitatively. The tensile test yielded parameters of ultimate tensile strength, yield strength, and elongation at break as indicators of mechanical strength. The hardness value was determined based on the average of five indentation points using the Brinell method. Microstructural observations were conducted to assess grain morphology and phase homogeneity. The corrosion test results were analyzed using the Tafel curve to obtain the corrosion rate of each sample. All data were compared between heat treatment conditions to determine the optimal treatment for geothermal turbine blade applications.

3. RESULTS AND DISCUSS

Brinell hardness testing was conducted on four SS 17-4 PH material conditions, namely H900, AVG, H1025, and as-cast. Each sample was tested at five points and the results were averaged to obtain a representative hardness value (Table 2, Figure 3).

Table 2. Brinell Hardness test results

Sample Name	Indentation location					Average Hardness (HRC)	Average Hardness (HB)
	1	2	3	4	5		
(A)	47,8	48,3	49	48,6	48,6	48,46	505,39
(B)	43,4	43,4	43,9	43,7	43,4	43,56	457,32
(C)	44,1	43,7	43,4	44,1	44,1	43,88	460,46
(D)	46,1	46,6	46,3	46,6	46,5	46,42	485,38

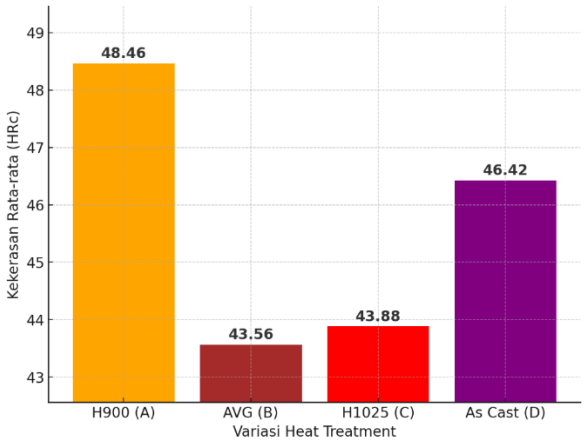

Figure 4. Material Hardness Comparison Graph

The results show that the H900 specimen has the highest hardness (505.39 HB) due to fine precipitates formed during heat treatment at 482°C. These precipitates effectively inhibit dislocation motion, increasing the strength and hardness of the material. In contrast, the AVG specimen exhibits a lower hardness (457.32 HB), indicating overaging due to enlarged and incoherent precipitates, thus reducing the resistance to dislocations.

The H1025 specimen also experienced a decrease in hardness (460.46 HB), caused by the precipitate coarsening process due to prolonged aging at high temperatures (550°C). This mechanism is followed by the possibility of recovery and formation of austenite, which reduces dislocation density and internal stress.

The as-cast sample exhibited a relatively high hardness (485.38 HB), supported by the dendritic microstructure and alloying element segregation that strengthened the matrix through solid solution and strain hardening. However, the absence of heat treatment resulted in a less homogeneous microstructure and potentially reduced ductility.

Overall, the H900 condition provides an optimal combination of hardness and microstructural control through uniform and fine precipitation, making it the most superior condition in terms of mechanical strength.

Tensile Test

Tensile testing was conducted on four heat treatment conditions of 17-4 PH stainless steel, namely H900, AVG (median value of tempering temperature and time parameters), H1025, and as-cast. Each condition was tested with three specimens and averaged to increase data reliability. Testing was conducted using a Universal Testing Machine (UTM) referring to the ASTM E8 standard, with the parameters analyzed including Ultimate Tensile Strength (UTS), Yield Strength (YS), Maximum Elongation, and Modulus of Elasticity.

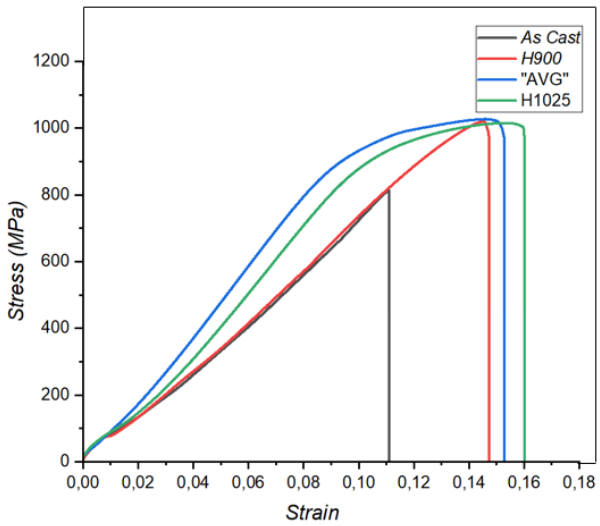

Figure 5. Stress strain curves at 4 heat treatment conditions

Table 3. Mechanical properties of 4 material conditions

Heat Treatment	*UTS (MPa)*	*YS (MPa)*	*Elongation (%)*	*Modulus Elastisity (MPa)*	*Hardness*	
					HRC	**HB**
H900 (A)	1007,87	939,249	4,81445	6756,033	48,46	505,39
AVG (B)	1031,59	844,412	7,27	10306,6	43,56	457,32
H1025 (C)	1021,82	860,907	7,08	9909,2	43,88	460,46
ascast (D)	812,73	-	2,52	7570,3	46,42	485,38

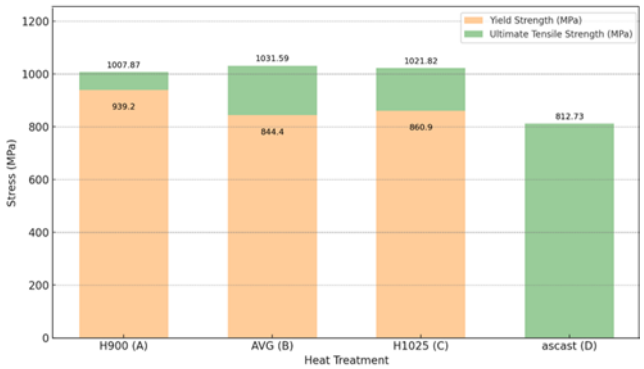

Figure 6. Comparison chart of UTS and YS 4 materials

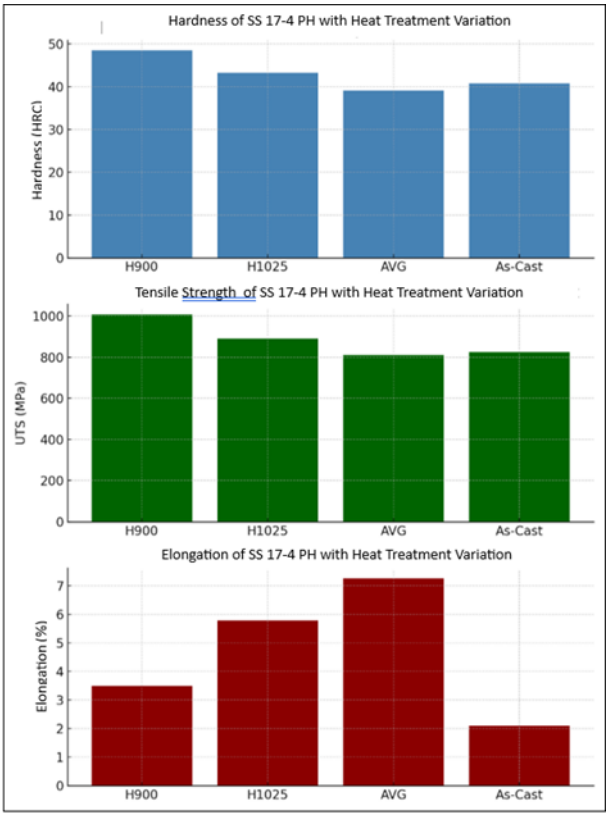

Figure 7. Mechanical Properties of 4 Material Variations

The results showed that the AVG (B) specimen had the highest UTS value (1031.59 MPa), followed by H1025 (1021.82 MPa) and H900 (1007.87 MPa). The as-cast specimen showed the lowest UTS value (812.73 MPa), indicating that tempering treatment plays an important role in increasing the tensile strength due to the formation of strengthening precipitates during the aging process. However, the highest YS value was recorded in the H900 condition (939.25 MPa), indicating the best ability to withstand elastic deformation. This achievement is associated with the distribution of fine precipitates that effectively inhibit dislocation motion, strengthening the metal matrix.

In terms of ductility, the AVG and H1025 specimens exhibited higher maximum elongation values (7.27% and 7.08%), compared to H900 (4.81%). This indicates that higher tempering temperatures and durations facilitated larger precipitate growth and reduced internal stress, thus enhancing the material's plastic deformation capability. In contrast, the as-cast specimen recorded the lowest elongation (2.52%), indicating a more brittle structure due to chemical segregation and microstructural irregularities that were not heat-treated.

In terms of stiffness, AVG has the highest elastic modulus (10306.6 MPa), followed by H1025 (9909.2 MPa) and H900 (6756.03 MPa). This value reflects that aging treatment at higher temperatures and times is able to increase the density of the martensite phase or rigid

intermetallic phase in the microstructure. Although the as-cast recorded a lower elastic value (7570.3 MPa) than AVG and H1025, the value is still in the moderate stiffness range, indicating a dendritic structure that still provides basic stiffness, although with low mechanical resistance and ductility.

Overall, the H900 treatment produced a material with the highest yield strength but limited ductility, while the AVG and H1025 treatments offered a compromise between strength and ductility. The as-cast condition showed the lowest mechanical performance across all parameters, highlighting the importance of heat treatment optimization in improving the mechanical properties of 17-4 PH stainless steel for high-temperature structural applications.

Metallography Test

Heat treatment of SS 17-4 PH begins with a solution treatment at 1050°C, resulting in a copper-saturated soft martensitic structure. The aging process forms a submicroscopic copper phase that strengthens the material through a precipitation hardening mechanism.

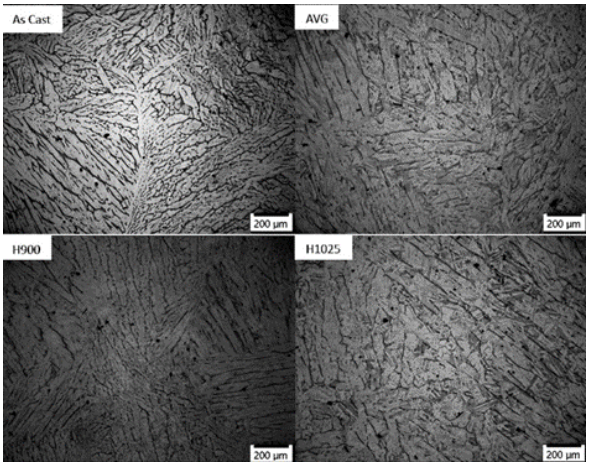

Figure 8. Microstructure at 100x magnification

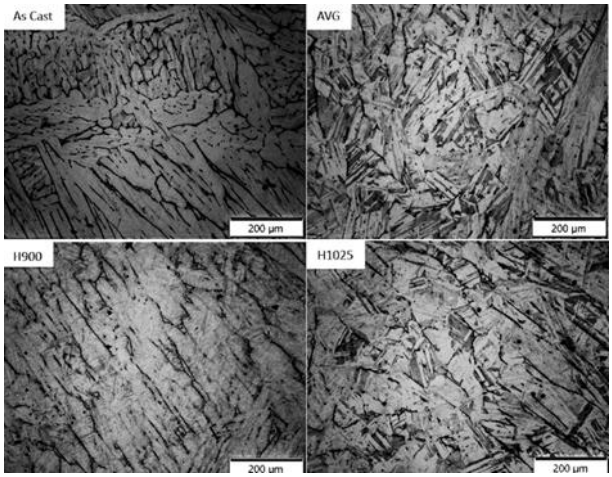

Figure 9. Microstructure at 200x magnification

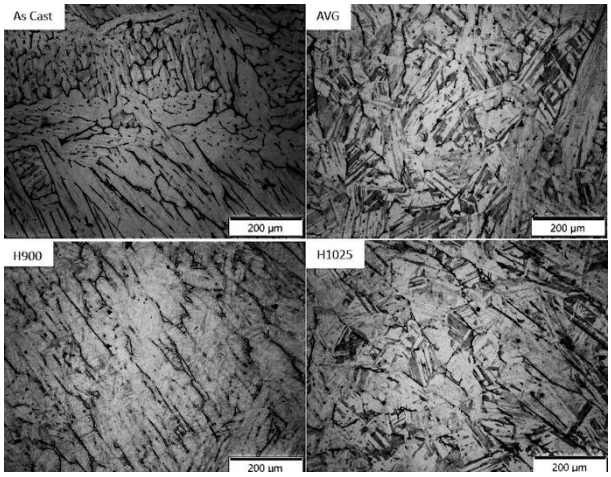

Figure 10. Microstructure at 500x magnification

Table 4. Porosity Percentage

Slice	Porosity Percentage (%)
as-cast-100x.tif	10.817
h900-100x.tif	11.384
avg-100x.tif	9.936
h1025-100x.tif	5.984

The as-cast microstructure exhibits coarse, elongated dendritic grains, typical of non-equilibrium solidification with high thermal gradients. This structure results in a non-uniform grain distribution and anisotropic mechanical properties. Porosity and non-metallic inclusions, such as oxides and sulfides, are abundant along grain boundaries and can potentially reduce tensile strength and fatigue resistance.

After H900 treatment, the dendritic morphology disappears, resulting in a smooth, uniform, tempered martensitic matrix. Solution treatment and air cooling reduce segregation and refine the structure. Porosity is drastically reduced, and inclusions are finely distributed. Precipitation of intermetallic compounds such as Cu and $Ni_3(Al,Ti)$ is uniformly distributed, strengthening the matrix by inhibiting dislocations. This structure exhibits good mechanical properties even without full martensite.

The "AVG" condition exhibits polygonal to elongated grains due to partial recrystallization. The grain size is intermediate between H900 and as-cast, with minimal porosity and inclusions. The lamellar and needle-like structures indicate martensite formation during air cooling. Fine precipitation effectively increases strength without signs of over-aging. Microstructural homogeneity is achieved, demonstrated by uniform grain contrast.

In the H1025 condition, a tempered martensitic structure forms through moderate cooling after austenitization and aging at 552°C. Precipitation of Cu, NiAl, and Cr carbides inhibits dislocations and increases hardness. The grains are polygonal with elongated martensite blades. Porosity is insignificant, while inclusions are finely dispersed without agglomeration.

In general, heat treatment improves microstructural homogeneity, reduces inclusions and porosity, and forms strengthening precipitation. These results make SS 17-4 PH treated with H900, AVG, and H1025 excellent candidates for high-temperature applications such as geothermal turbine blades.

Corrosion Test (Potentiodynamic Polarization)

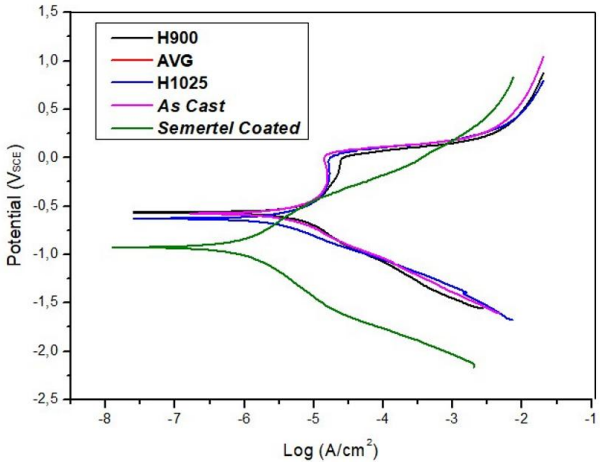

Figure 11. Potentiodynamic Polarization Curve

Table 5. Comparative Data of Corrosion Parameters of SS 17-4 PH 5 conditions

SS 17-4 PH	Ecorr (mv)	Icorr (µA)	βa (mv)	βc (mv)	Chi-square	Corrosion Rate (mpy)	Corrosion Rate (mm/y)
(A)	-565,506	4,909	373,264	379,405	122,67	2,0841	0,053
(B)	-742,747	7,077	463,467	344,514	55,603	3,0045	0,076
(C)	-627,779	2,526	360,998	290,065	1082,2	1,0724	0,027
(D)	-580,441	3,608	407,251	335,865	208,34	1,5319	0,039
(E)	-927,354	774,698	406,922	364,402	25,031	0,32887	0,008

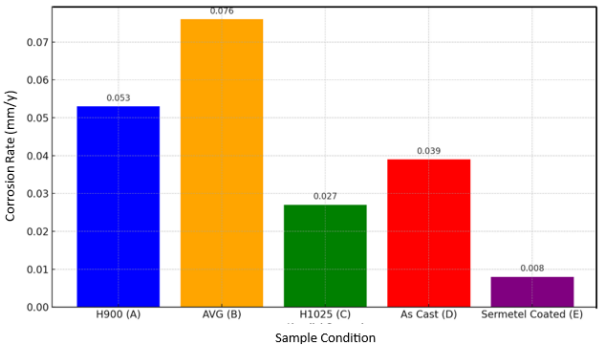

Figure 12. Comparison graph of corrosion rates for 5 material conditions

Based on the results of corrosion tests using the potentiodynamic polarization method, the H1025 heat treatment variation showed the best corrosion resistance performance compared to the H900, AVG, and as-cast variations. This is indicated by the lowest corrosion current (Icorr) value of 2.526 µA and a corrosion rate of only 0.027 mm/y, indicating that the rate of electrochemical reactions that damage the material runs the slowest. The relatively negative Ecorr value of -627.779 mV also indicates a more stable passivation tendency.

The higher corrosion resistance in the H1025 condition is closely related to the microstructure resulting from aging at 552°C. In this condition, the precipitation of intermetallic compounds such as Cu-rich phases and NiAl is formed stably and evenly distributed in the tempered martensitic matrix. The presence of these fine precipitates not only strengthens the structure but also blocks the diffusion path of aggressive ions such as Cl in the brine fluid, which is commonly found in the environment of PLTP (Geothermal Power Plant). In addition, the homogeneity of the grains and the reduction of porosity and inclusions in the microstructure also strengthen the protection against local corrosion such as pitting and intergranular attack.

In contrast, the H900 condition, despite its superior hardness and mechanical strength, exhibited a higher corrosion rate of 0.053 mm/y. This is likely due to the presence of internal residual stresses and inclusions that have not been completely removed despite the relatively fine precipitation. The H900 microstructure also has a wider active zone for redox reactions due to the less uniform distribution of surface energy chemically.

Under AVG conditions, the highest Icorr value (7.077 µA) and the highest corrosion rate (0.076 mm/y) indicate that precipitation that begins to experience over-aging actually reduces corrosion resistance. This is in accordance with microstructural observations that show coarser precipitate growth and reduced effectiveness of dislocation inhibition and electrochemical protection.

The As-Cast sample ranks between AVG and H900 in terms of corrosion rate (0.039 mm/y), but its coarse dendritic structure, high porosity, and inhomogeneous inclusions make it less suitable for long-term applications in corrosive environments.

Considering the corrosion performance and support from the microstructure results, the H1025 heat treatment is the most ideal choice for geothermal power plant applications, because it is able to balance mechanical strength with superior corrosion resistance in aggressive geothermal environments.

4. CONCLUSION

Based on the evaluation results of the performance of 17-4 PH stainless steel resulting from the investment casting process with three heat treatment variations (H900, H1025, and AVG) according to the ASTM A747 standard, it can be concluded that the heat treatment conditions have a significant influence on the mechanical properties, corrosion resistance, and microstructure of the material. The H900 heat treatment is proven to produce the highest hardness and tensile strength, making it superior for applications that require high strength. On the other hand, the H1025 condition provides the highest elongation and the best corrosion resistance, indicating its suitability for applications that require ductility and stability at high temperatures. Meanwhile, the AVG condition provides a balanced combination of strength, ductility, and corrosion resistance, making it an adaptive alternative to the complex load conditions in geothermal power plant turbine systems.

Thus, the optimal heat treatment is determined based on the specific needs of the geothermal turbine components. Where maximum structural strength is required, H900 is the preferred choice, while H1025 is more suitable for components subject to temperature fluctuations and long-term thermal deformation, such as the blade root or turbine disc. Overall, the results support the potential use of locally produced 17-4 PH stainless steel as a substitute for imported materials in the development of geothermal turbine components, in line with efforts to strengthen national energy independence.

THANKS

The author expresses praise and gratitude to God Almighty for all His grace and gifts so that the author can complete this research well. With utmost respect and sincerity, the author expresses his deepest gratitude to his supervisors, Dr. Riri Murniati, S.Si., M.Si. and Dr. Ir. Agus Hadi Santoso W., S.T., M.Sc., for their guidance, direction, and knowledge throughout

the writing process. The patience, thoroughness, and support of their supervisors have been crucial to the successful completion of this work.

The author also expresses gratitude to the National Research and Innovation Agency (BRIN) for providing research opportunities and facilities, as well as for being a platform supporting the development of science and research. BRIN's presence as a national research institution has significantly contributed to the smooth implementation of this research.

Finally, the author realizes that this paper is far from perfect. Therefore, any constructive input and criticism is greatly appreciated for future improvements.

REFERENCES

Aristia, G., Hoa, L. Q., & Bäßler, R. (2025). Corrosion of carbon steel in artificial geothermal brine: Influence of carbon dioxide at 70 °C and 150 °C. *Materials*, *12*(22), 3801. https://doi.org/10.3390/ma12223801

Azhar, M., & Satriawan, D. A. (2018). Implementasi kebijakan energi baru dan energi terbarukan dalam rangka ketahanan energi nasional. *Online Administrative Law & Governance Journal, 1*.

Batubara, M. (2018). *Pengembangan panas bumi: Sebagai energi kearifan lokal di Indonesia*. Yayasan Pengkajian Sumber Daya Indonesia.

Bertani, R. (2016). Geothermal power generation in the world 2010–2014 update report. *Geothermics, 60*, 31–43.

Blecich, A. A., & Blecich, P. (2021). Factors affecting the cost of electricity from geothermal power plants. *Innovations*.

IEA. (2021). *World energy outlook 2021*. International Energy Agency.

Iglesias, N., & Díaz, E. (2025). Influence of H_2S and CO_2 partial pressures and temperature on the corrosion of superduplex S32750 stainless steel. *Corrosion and Materials Degradation, 6*(2), 20. https://doi.org/10.3390/cmd6020020

IPCC. (2018). *Global warming of 1.5°C*. Intergovernmental Panel on Climate Change.

Kabeyi, M. J. B., & Olanrewaju, O. A. (2021). Central versus wellhead power plants in geothermal grid electricity generation. *Energy, Sustainability and Society, 11*, 7.

Karlsdottir, S. N., Thorbjornsson, I. O., & Einarrson, A. (2015). Corrosion testing in superheated geothermal steam in Iceland.

Karthik, D., Kalainathan, S., & Swaroop, S. (2015). Surface modification of 17-4 PH stainless steel by laser peening without protective coating process. *Surface and Coatings Technology, 278*, 138–145. https://doi.org/10.1016/j.surfcoat.2015.08.012

Penot, C., Martelo, D., & Paul, S. (2023). Corrosion and scaling in geothermal heat exchangers. *Applied Sciences, 13*(20), 11549. https://doi.org/10.3390/app132011549

Sabooni, S., Chabok, A., Feng, S. C., Blaauw, H., Pijper, T. C., Yang, H. J., & Pei, Y. T. (2021). Laser powder bed fusion of 17–4 PH stainless steel: A comparative study on the effect of heat treatment on the microstructure evolution and mechanical properties. *Additive Manufacturing, 46,* 102176. https://doi.org/10.1016/j.addma.2021.102176

Trisakti, B., Sidabutar, R., Lumbangaol, A. K., Lumbangaol, A. K., Hutagalung, A., Lumbangaol, P., & Irvan. (2020). Effect of sulphuric acid (H_2SO_4) and sodium hydroxide (NaOH) addition to prevent silica scaling in geothermal power plant projection pipes at PLTP X. *IOP Conference Series: Materials Science and Engineering, 801*(1), 012038. https://doi.org/10.1088/1757-899X/801/1/012038

Wyszomierski, R., Bórawski, P., Bełdycka-Bórawska, A., Brelik, A., Wysokiński, M., & Wiluk, M. (2025). The cost-effectiveness of renewable energy sources in the European Union's ecological economic framework. *Sustainability, 17*(10), 4715. https://doi.org/10.3390/su17104715

Yamamoto, Y., Miyazaki, M., & Watanabe, M. (n.d.). Turbine materials for geothermal power generation. Toshiba Corporation.

Zarrouk, S. J., & Moon, H. (2014). Efficiency of geothermal power plants: A worldwide review. *Renewable and Sustainable Energy Reviews, 30,* 101–125.